Neoplasma 2024; 71(6): 581–593

doi:10.4149/neo_2024_240604N243

hsa_circ_0021727 facilitates esophageal squamous cell carcinoma progression by stabilizing GBX2 mRNA through interacting with EIF4A3

Jie LIN[1], Qiuping ZHU[1], Fanlin ZENG[2,*]

[1]*Department of Intensive Medicine/Comprehensive Intensive Care Unit, The First Affiliated Hospital of Gannan Medical University, Ganzhou, Jiangxi, China;* [2]*Department of General Surgery/Hepatobiliary and Pancreatic Surgery, The First Affiliated Hospital of Gannan Medical University, Ganzhou, Jiangxi, China*

**Correspondence: zengfanlin5210@163.com*

Received June 4, 2024 / Accepted December 16, 2024

Esophageal squamous cell carcinoma (ESCC) has high mortality. The role and regulatory mechanism of hsa_circ_0021727 (circ_0021727) in ESCC remain largely unknown. This study focused on the undiscovered impact of circ_0021727 on cell cycle progression, apoptosis, and angiogenesis of ESCC. We found that circ_0021727 levels were significantly upregulated in ESCC cells. TUNEL, flow cytometry, and tubule formation assay indicated that knockdown of circ_0021727 in ESCC induced cell arrest at the G0/G1 phase, promoted apoptosis, and inhibited angiogenesis, whereas overexpression of circ_0021727 produced the opposite effect. Gastrulation brain homeobox 2 (GBX2) GBX2 was a downstream target gene of circ_0021727, and overexpression of GBX2 reversed the effect of circ_0021727 knockdown in ESCC progression. The results of the RIP and RNA pull-down showed that circ_0021727 and GBX2 mRNA bound with eukaryotic translation initiation factor 4A3 (EIF4A3). Overexpression of circ_0021727 promoted GBX2 mRNA stability by binding with EIF4A3. In a tumor xenograft model, the knockdown of circ_0021727 inhibited tumor growth, which was reversed by further overexpression of GBX2. In conclusion, circ_0021727 increased GBX2 mRNA stability by recruiting EIF4A3, which promoted cell cycle progression and angiogenesis in ESCC.

Key words: esophageal squamous cell carcinoma; cell cycle arrest; angiogenesis; hsa_circ_0021727; GBX2

The esophageal squamous cell carcinoma (ESCC) is a common digestive system tumor that is usually diagnosed at a later stage, frequently metastasizes, and exhibits a high tendency for recurrence, and therapy resistance [1, 2]. Despite previous improvements in ESCC treatment, the high incidence and low survival rates of ESCC remain a public health concern [3]. The molecular mechanism underlying the development of ESCC remains to be fully elucidated. It is urgently needed to determine the exact molecular mechanism of ESCC pathogenesis to provide a theoretical basis for the clinical treatment of ESCC.

CircRNA, unlike linear RNA, consists of a covalent closed-loop structure [4, 5]. It has been extensively documented that circRNA dysregulation is associated with various types of cancer, including ESCC [5–8]. hsa_circ_0021727 is generated by the host CD44 gene, which was spliced from exon 8 to 10. In our previous research, we identified that an abnormally overexpressed circ_0021727 promoted the invasion, migration, and proliferation of ESCC through TAK1 binding protein (TAB1)/nuclear factor-κB (NF-κB) signaling [9]. However, the effects of circ_0021727 on the ESCC cell cycle, apoptosis, and angiogenesis have not been reported. Therefore, our aim was to investigate in more depth the effect and molecular mechanism of circ_0021727 on these functions in ESCC cells.

CircRNA can interact with RNA-binding proteins (RBPs) and subsequently participate in the transcription and expression of tumor-related genes [10, 11]. Eukaryotic translation initiation factor 4A3 (EIF4A3) is a core protein of the exon ligation complex involved in RNA splicing, decay, translation, and localization [12]. EIF4A3 is an RBP that has been discovered to interact with circRNAs in various cancer cells, ultimately affecting downstream mRNA stability. For example, circKIF4A interacted with EIF4A3 to stabilize the expression of stearoyl-CoA desaturase 1 (SDC1) and promote the progression of triple-negative breast cancer [13]. Circ-USP9X interacted with EIF4A3 to enhance the stability of gasdermin D (GSDMD) to promote ox-LDL-induced

pyrolysis of human umbilical vein endothelial cells [14]. In addition, we identified the potential binding of circ_0021727 to EIF4A3 through CircInteractome and starBase databases. Therefore, we speculated that circ_0021727 might bind to EIF4A3 to regulate downstream genes and affect ESCC development.

Gastrulation brain homeobox 2 (GBX2) is a transcription factor containing homeobox that promotes the development of cancer [15]. GBX2 not only exacerbates the progression of laryngeal, lung, and breast cancers but also promotes tumor deterioration in the digestive system [15–18]. For example, elevated GBX2 levels shorten the overall survival of gastric cancer patients [17]. GBX2 also enhanced the viability of hepatoma cells and inhibited apoptosis [18]. Importantly, we found that GBX2 is highly expressed in ESCC through the starBase database. This suggested that GBX2 may also play a pro-cancer role in ESCC. It is worth noting that we found that EIF4A3 and GBX2 mRNA were positively correlated in ESCC through the starBase database, and there was a possibility of mutual binding between EIF4A3 protein and GBX2 mRNA. However, whether EIF4A3 binding to GBX2 affects GBX2 mRNA stability, which in turn affects ESCC cell cycle, apoptosis, and angiogenesis, needs further investigation.

In conclusion, we investigated the role of circ_0021727 in ESCC cell cycle arrest, angiogenesis, and apoptosis. Through an in-depth study of its molecular mechanism, we hope to contribute new theoretical knowledge to ESCC.

Materials and methods

Cell culture. ESCC cells (KYSE510 and TE-1) and human esophageal epithelial cell line (Het-1A) were initially cultured in RPMI-1640 medium (Biological Industries) supplemented with 10% fetal bovine serum (FBS) (Gibco, Grand Island, NY, USA). The cells were maintained in a 37 °C, 5% CO_2 incubator. Human umbilical vein endothelial cells (HUVECs) were cultured in an endothelial growth medium (ScienCell, Carlsbad, CA, USA), which was supplemented with 5% FBS. TE-1 cells were obtained from the Cell Resource Center of the Shanghai Institute of Life Sciences, Chinese Academy of Sciences, and KYSE510 cells from FuXiang Biotechnology (Shanghai, China). HUVECs and Het-1A cells were purchased from the American Type Culture Collection (Manassas, VA, USA).

Table 1. The primer sequences.

Primers	Sequences (5'–3')
GBX2	F: CCGCCTTCAGCATAGACTCG
	R: GGTAGCCGGTGTAGACGAAAT
EIF4A3	F: AAGGGAGAGATGTCATCGCAC
	R: GCTTGAGTTTCACGAACCTGA
CD44	F: CACCACGGGCTTTTGACCAC
	R: TGAATGAGGGGAGGGTGTGC
hsa_circ_0021727	F: CAGAAGGAACAGTGGTTTGG
	R: TCCGGATTTGAATGGCTTGG
GAPDH	F: GGAGCGAGATCCCTCCAAAAT
	R: GGCTGTTGTCATACTTCTCATGG

Cell transfection. The circ_0021727 and GBX2 genes were cloned into pcDNA3.1 and pcDNA3.1 circRNA mini vectors to construct overexpressed GBX2 (oe-GBX2) and plasmids circ_0021727 (oe-circ_0021727), respectively. The corresponding empty vector was used as a negative control (oe-NC). Short hairpin RNAs (shRNAs) of circ_0021727 (sh-circ_0021727#1: 5'-CTTTTGACCACA-CAAAACAGA-3', sh-circ_0021727#2: 5'-GGGACAGCT-GTTTCAACCACA-3'), EIF4A3 (sh-EIF4A3: 5'-GCAAT-CAAGCAGATCATCAAA-3'), and GBX2 (sh-GBX2: 5'-GCTTCGCTCGGCCGCCTCTGC-3') were cloned into the pGPU6/GFP/Neo vector (C02007, GenePharma, Shanghai, China) and its empty vector was used as a negative control. The above plasmids were transfected into TE-1 and KYSE510 cells using Lipofectamine™ 3000 (Thermo Fisher Scientific). The transfection efficiency was detected by immunofluorescence 48 hours later. The knockdown or overexpression effect was assessed by real-time quantitative PCR and western blot after transfection efficiency reached more than 90%.

Real-time quantitative PCR (RT-qPCR). Total RNA was extracted from cells using TRIzol (Takara, Dalian, China) reagent, and cDNA was synthesized using PrimeScript™ RT reagent Kit (Takara). Circ_0021727, GBX2, and EIF4A3 mRNA levels were detected by TB Green® Premix Ex Taq™ II (Takara). The expression of each gene was calculated by $2^{-\Delta\Delta Ct}$. The primer sequences are shown in Table 1.

Western blot. TE-1 and KYSE510 cells were lysed using RIPA lysis buffer supplemented with phenylmethanesulfonylfluoride (PMSF) (Solarbio, Beijing, China). Then, the protein samples were quantified by the BCA kit (#P0010, Beyotime, Shanghai, China). The equal protein samples (30 μg) were separated on SDS-PAGE, and then the proteins were transferred to the PVDF membrane. Afterwards, proteins were blocked with 5% skim milk powder and incubated with primary antibodies: GBX2 (1:2000, #ab227853, Abcam, Manassas, VA, USA), EIF4A3 (1:2500, #ab180573, Abcam), Cyclin D1 (1:200, #ab16663, Abcam), CDK6 (1:50000, #ab124821, Abcam), and GAPDH (1:10000, #2118, CST, Boston, MA, USA) overnight at 4 °C. Then, it was incubated with IgG (1:10000, #ab6721, Abcam) for 2 h at 25 °C. Protein bands were detected with chemiluminescent substrates (Meilunbio, Dalian, China) for luminescence. GAPDH was then used as a normalization control. Protein bands were then quantified using ImageJ software (GE Healthcare, Sunnyvale, CA, USA).

CCK-8 assay. TE-1 and KYSE510 cells were seeded on 48-well plates, respectively. Each well contained 3,000 cells/100 μl of medium. Each well of the cell culture was supplemented with CCK-8 solution (10 μl) (Meilunbio, Dalian, China). Following this, the cells were incubated for a

further 4 hours, and the absorbance at 450 nm was measured at regular intervals of 24, 48, 72, and 96 h.

Terminal dexynucleotidyl transferase (TDT)-mediated dUTP nick end labeling (TUNEL) assay. After collection, cells were fixed to a glass slide using a specialized method using 4% paraformaldehyde for 30 min. Subsequently, they were incubated in PBS (containing 0.3% Triton X-100). According to the One Step TUNEL Apoptosis Assay Kit (Beyotime) guidelines, a biotin labeling solution with a 1:9 ratio of TdT enzyme to Biotin-dUTP was prepared. Biotin labeling solution was participated in the sample and cultivated at 37 °C for 60 min. Subsequently, the labeling reaction termination was added and incubated for 10 min. The apoptotic state was determined by assessing the proportions of TUNEL-positive cells in each microscopic field under a fluorescence microscope (DM2500, Leica, Wetzlar, Germany).

Flow cytometry. Successfully transfected ESCC cells were digested and transferred to a centrifuge tube. After the solution was centrifuged and the supernatant was discarded, pre-cooled PBS was added. It was then fixed with 75% ice ethanol for 24 h and centrifuged again. Cells were treated at room temperature for 30 minutes in the dark with propidium iodide (PI) (ShareBio, Shanghai, China). Finally, DNA content in cells of S, G2/M, and G0/G1 phases was detected by FACS Calibur Flow Cytometer (BD Biosciences, San Jose, CA, USA).

For apoptosis, it was measured using the Annexin V-FITC Apoptosis Detection Kit (Beyotime). The treated cells were digested using 0.25% trypsin. The cell precipitate was collected after centrifugation. Cells were resuspended using 1× Annexin Binding Buffer at a concentration of 1×10^6 cells/ml. Subsequently, the cells were incubated with 10 µl Annexin V-FITC and 5 µl PI for 15 min away from light. Detection was carried out on a flow cytometer within 1 h, and the data were analyzed using the software. Apoptosis was detected within 1 h using a FACS Calibur flow cytometer (BD Biosciences).

HUVECs tube formation assay. 96-well plates were pre-cooled before adding a Freeze-thawed Matrigel (Corning, NY, USA). When HUVECs were grown to 70–80%, they were digested. Digestive juices were suspended with DMEM containing 10% FBS, and the number of cells was counted. The resuspension was added to a plate containing with Matrigel, following the incubation at 37 °C. Endothelial cell angiogenesis was quantified using the software ImageJ.

RNA immunoprecipitation (RIP) assay. The binding relationships of circ_0021727 to EIF4A3 and GBX2 to EIF4A3 were detected by Merck17-700 Magna RIP Kit in Merck Millipore (Billerica, USA). TE-1 and KYSE510 cells were lysed. Then the protein lysate was incubated with anti-EIF4A3 (1:1000, #ab180573, Abcam) or anti-IgG (1:100, #ab172730, Abcam) overnight at 4 °C. Then, the A/G protein magnetic beads were added and incubated at 4 °C for 4 h. Protease K was used for digestion, and RNA was extracted for subsequent RT-qPCR detection.

RNA pull-down assay. Biotinylated probes circ_0021727 and GBX2 were designed and produced by RiboBio (Guangzhou, China). We incubated TE-1 and KYSE510 cells with biotin-labeled scramble or circ_0021727 targeting probes, respectively, for 2 h. Afterward, cells were treated with streptavidin magnetic beads for 1 h (Life Technologies, Carlsbad, CA, USA). The beads were washed 5 times repeatedly to elute the bound protein and analyzed by western blot.

Dual-luciferase reporter gene assay. The presence of binding sites for miR-23b-5p and GBX2 mRNA was predicted by the TargetScan database. The binding site sequence fragments of wild type (WT) and mutant (MUT) of GBX2 were designed and cloned into the firefly luciferase gene in the pGL3 promoter vectors. GBX2-WT/GBX2-MUT plasmids and miR-23b-5p mimics/miR-23b-5p inhibitor or NC were co-transfected into KYSE510 or TE-1 cells. After 48 h of incubation, luciferase activity was assayed using the dual-luciferase reporter assay system (E1910, Promega). The ratio of fluorescence intensity of firefly luciferase to that of Renilla luciferase was normalized for each sample with reference to the control.

GBX2 mRNA stability detection. Cells were exposed to 5 µg/ml of actinomycin D (Sigma, St. Louis, MO, USA) for 0, 3, 6, 9, and 12 h, and then total RNA was collected. The expression of the remaining GBX2 mRNA was detected by RT-qPCR.

Subcutaneous transplanted tumor. BALB/c male nude mice of 4–5 weeks of age weighing about 15–18 g were purchased from SJA Laboratory Animal Co. Ltd (Hunan, China). All nude mice were housed in SPF-grade animal rooms (relative humidity of 55±5%, temperature of 24.0±2.0 °C, and alternating cycles of light/dark for 12 h). Nude mice were divided into Control, sh-NC+oe-NC, sh-circ_0021727+oe-NC, and sh-circ_0021727+oe-GBX2 groups (n=6). Lentiviral vectors packaged with sh-NC, sh-circ_0021727, oe-NC, and oe-GBX2 were co-transfected into 293T cells for 48 h using Lipofectamine™ 3000 (Thermo Fisher Scientific). The supernatant of the cells was collected, concentrated, and purified. KYSE510 cells (1×10^6 cells) were infected with the virus solution (2.0×10^8 TU/ml). KYSE510 cells successfully infected with lentivirus were screened with 2 µg/ml puromycin (InvivoGen, San Diego, CA, USA). After 7 days of environmental acclimatization, 1 ml of lentivirus-infected KYSE510 cell suspension was injected subcutaneously into the right arm of the nude mice. The control group was injected with the same volume of saline. Tumor volumes were measured and recorded every 5 days from the date of inoculation. Nude mice were executed by spinal dislocation 25 days after tumor formation. Subsequently, the subcutaneous rhabdomyosarcoma was peeled off, photographed, and weighed. Animal experiments were approved by The Animal Ethics Committee of The First Affiliated Hospital of Gannan Medical University.

Immunohistochemical detection (IHC). Fresh tumor tissues were washed with PBS and then fixed for 24 hours

using 4% paraformaldehyde. After the tissue was dehydrated, it was embedded using paraffin. The paraffin blocks were then sectioned using a slicer (4 mm). Next, the sections were immersed in xylene to dewax. Then, antigen repair was performed using citrate buffer. Non-specific binding proteins were blocked using 5% goat serum. The sections were then incubated overnight with anti-Ki-67 antibody (1:200, #ab16667, Abcam) and anti-CD31 antibody (1:50, #ab28364, Abcam), respectively. The next day, sections were incubated with goat anti-rabbit IgG (1:200, #ab150077, Abcam) for 1 h. Subsequently, the color was visualized with DAB chromogen, and the nuclei were stained with hematoxylin. After sealing the slices with neutral resin, images were captured using an inverted microscope (Olympus, Tokyo, Japan), and protein expression was analyzed under ImageJ software.

Bioinformatics analysis. The starBase database (https://starbase.sysu.edu.cn/index.php) was used to predict GBX2 expression in ESCC and the correlation between EIF4A3 and GBX2 expression. The potential binding of circ_0021727 to EIF4A3 was predicted by CircInteractome (https://circinteractome.nia.nih.gov/) and the starBase database. The presence of binding sites for miR-23b-5p and GBX2 mRNA was predicted by the TargetScan database (http://www.targetscan.org/vert_80/).

Statistical analysis. All raw data were analyzed using statistical analysis software and presented as mean ± standard deviation. All experiments were repeated at least 3 times. The Student's t-test or one-way analysis of variance (ANOVA) was used for comparing the variance between two or multiple groups, respectively. A p-value <0.05 indicated statistically significant.

Results

circ_0021727 promoted cell cycle progression and angiogenesis and inhibited apoptosis of ESCC cells. Firstly, we examined the role of circ_0021727 in ESCC cells. Circ_0021727 originated from the CD44 gene, which is spliced from exons 8 to 10 (Figure 1A). Then RT-qPCR experiments were performed. The results showed that circ_0021727 expression in ESCC cells (KYSE510 and TE-1) was significantly increased compared to human esophageal epithelial cells Het-1A (Supplementary Figure S1A). Next, sh-circ_0021727#1, sh-circ_0021727#2, or oe-circ_0021727 were transfected into the ESCC cells for circ_0021727 knockdown or overexpression, respectively. The transfection efficiency of sh-circ_0021727#1 (later named sh-circ_0021727) and oe-circ_0021727 reached more than 90% and were used for subsequent detection (Supplementary Figure S1B). sh-circ_0021727 was found to decrease circ_0021727 level, while oe-circ_0021727 vectors markedly overexpressed circ_0021727 (Supplementary Figure S1C). Moreover, knockdown or overexpression of circ_0021727 did not affect the mRNA level of its host gene CD44 (Supplementary Figure S1D). In addition, we heeded that the knockdown of circ_0021727 inhibited ESCC cells' viability (Supplementary Figure S1E) and promoted apoptosis (Figure 1B, Supplementary Figure S1F) while boosting circ_0021727 expression had the opposite effect. In addition, the knockdown of circ_0021727 significantly increased the proportion of ESCC cells in the G0/G1 phase compared with the sh-NC group. However, overexpression of circ_0021727 significantly decreased the proportion of ESCC cells in the G0/G1 phase compared with the oe-NC group (Figure 1C). Meanwhile, circ_0021727 knockdown decreased the expression of cell cycle-related proteins (cyclin D1 and CDK6), and overexpression of circ_0021727 showed the opposite effect (Figure 1D). What's more, we observed that the knockdown of circ_0021727 inhibited HUVEC tubule formation, while the overexpression of circ_0021727 enhanced this process (Figure 1E). The above results suggested that high expression of circ_0021727 facilitated the cell cycle progression and angiogenesis and suppressed the apoptosis of ESCC cells.

GBX2 was the downstream factor of circ_0021727. GBX2 is an important cancer-promoting factor, which involved in the invasion and migration of cancer cells [16]. The cancer-promoting effects of GBX2 in digestive system cancers such as gastric cancer and hepatocellular carcinoma suggest that GBX2 may also play a role in ESCC. As shown in Figure 2A, starBase database evidenced that GBX2 was strongly expressed in ESCC. RT-qPCR and western blot results also indicated that GBX2 was significantly upregulated in ESCC cells (Figures 2B, 2C). Next, we further speculated whether GBX2 was regulated by circ_0021727. Furthermore, we investigated the effect of knockdown or overexpression circ_0021727 on GBX2 expression levels in ESCC cells. Knockdown of circ_0021727 remarkedly decreased the mRNA and protein levels of the GBX2 (Figures 2D, 2E). Conversely, overexpression of circ_0021727 notably elevated GBX2 expression (Figures 2F, 2G). Collectively, these results revealed that circ_0021727 had a positive regulatory effect on the expression of GBX2, which was a downstream target gene of circ_0021727 in ESCC cells.

circ_0021727 stabilized GBX2 mRNA by recruiting EIF4A3. Next, we further explored how circ_0021727 regulates GBX2. Given that circular RNAs can regulate mRNA stability by sponging miRNAs. And our previous study found that hsa_circ_0021727 mainly targeted to regulate miR-23b-5p in ESCC [9]. However, whether hsa_circ_0021727 can affect GBX2 mRNA expression through miR-23b-5p sponging is unknown. We predicted the binding sites for miR-23b-5p and GBX2 mRNA by the TargetScan database (Supplementary Figure S2A). However, further dual-luciferase reporter gene assay did not find the binding of miR-23b-5p and GBX2 mRNA (Supplementary Figure S2B). The above results suggested that hsa_circ_0021727 might not be able to influence the stability of GBX2 mRNA through miR-23b-5p sponge function. CircRNAs also play an important role in cancer development through interacting with RBPs to regulate target gene mRNA

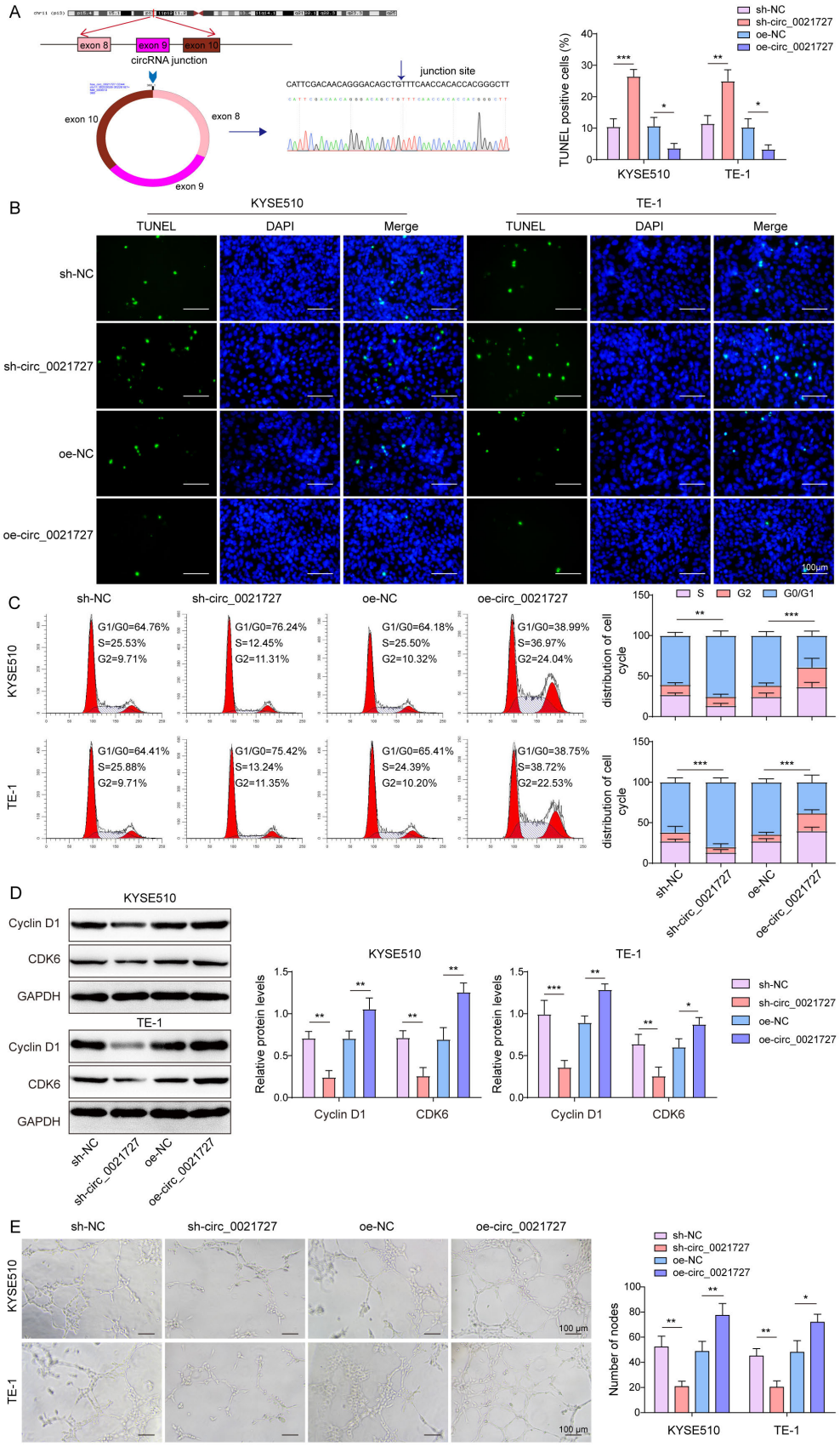

Figure 1. circ_0021727 promoted cell cycle progression and angiogenesis and inhibited apoptosis of ESCC cells. A) Schematic diagram of the structure of the circ_0021727. B) TUNEL assay detected the effect of knockdown or overexpression of circ_0021727 on apoptosis of ESCC cells. The bar graph displayed the statistics of the percentage of TUNEL-positive cells. Scale bar = 100 μm C) The cell cycle distribution of ESCC after knockdown or overexpression of circ_0021727 was resolved by flow cytometry. D) Western blot was used to detect the cycle-associated proteins cyclin D1 and CDK6 expression in ESCC cells with knockdown or overexpression circ_0021727. E) Detection of angiogenesis of HUVECs by tubule formation assay after knockdown or overexpression of circ_0021727. Scale bar = 100 μm; n=3/group; *p<0.05, **p<0.01, p<0.001

stability, so we then analyzed RBPs with the possibility of binding to circ_0021727 through starBase and CircInteractome databases. Among them, 95 candidate RBPs were displayed in the starBase database, while only 3 were in the CircInteractome database. It is worth noting that EIF4A3 is the RBP of GBX2 mRNA jointly revealed by starBase and CircInteractome databases (Figure 3A). RNA pull-down and RIP experiments also showed that circ_0021727 and EIF4A3 are bound to each other in KYSE510 and TE-1 cells (Figures 3B, 3C). Interestingly, the starBase database analysis revealed a positive correlation between EIF4A3 and GBX2 mRNA in ESCC (Figure 3D). At the same time, the binding relationship between GBX2 mRNA and EIF4A3 was demonstrated (Figures 3E, 3F). Since circRNA can maintain the stability of downstream mRNA by recruiting EIF4A3 [13, 19], we further performed knockdown treatment on EIF4A3 to determine whether it affected the stability of GBX2 mRNA. As seen in Supplementary Figures S3A–S3C, EIF4A3 was successfully knocked down after transfection of sh-EIF4A3. Knockdown of EIF4A3 decreased the stability of GBX2 mRNA (Figure 3G). Besides, after the knockdown of circ_0021727, the binding effect of GBX2 to EIF4A3 was weakened (Figure 3H). More importantly, overexpression of circ_0021727 could promote the stability of GBX2 mRNA, which was abolished by the knockdown of EIF4A3 (Figure 3I). In conclusion, circ_0021727 promoted GBX2 mRNA stabilization by combining with EIF4A3.

Knockdown of GBX2 inhibited cell cycle progression and angiogenesis and promoted apoptosis in ESCC cells. To elucidate the effects of GBX2 on ESCC cells, we trans-

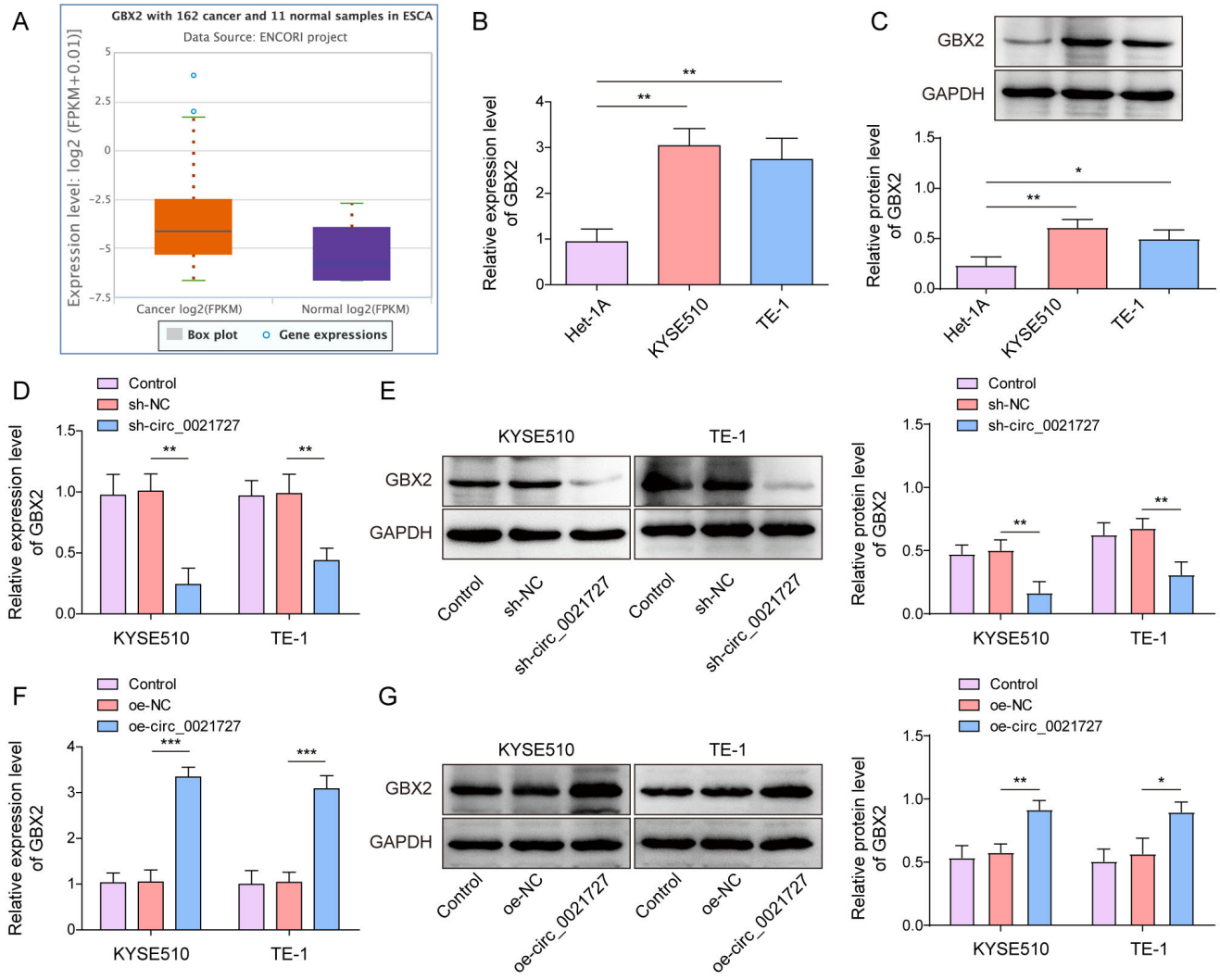

Figure 2. GBX2 was the downstream factor of circ_0021727. A) Prediction of GBX2 expression in ESCC by starBase database. B, C) GBX2 mRNA levels in Het-1A, KYSE510, and TE cells were detected by RT-qPCR and western blot. D, E) GBX2 expression was detected by RT-qPCR and western blot after knocking down circ_0021727. F, G)GBX2 levels in ESCC cells were measured by RT-qPCR and western blot after overexpressing circ_0021727. n=3/group; *p<0.05, **p<0.01, p<0.001

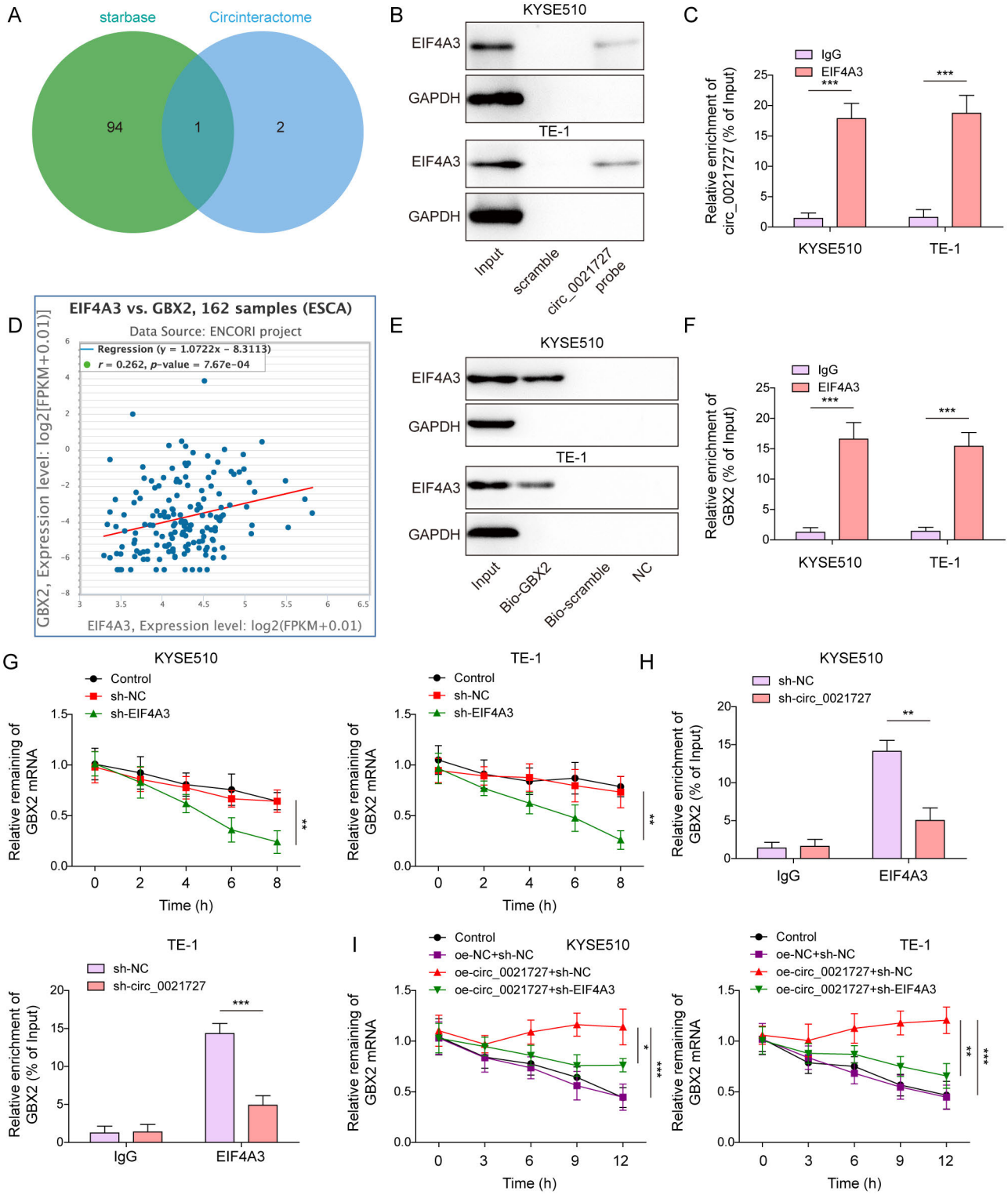

Figure 3. circ_0021727 stabilized GBX2 mRNA by recruiting EIF4A3. A) starBase and CircInteractome databases analyzed RBPs that combined with circ_0021727. B, C) RNA pull-down and RIP were utilized to evaluate the binding relationship between circ_0021727 and EIF4A3 in ESCC cells, respectively. D) The starBase database predicted the relationship between EIF4A3 and GBX2 in esophageal cancer. E, F) The binding relationship between GBX2 mRNA and EIF4A3 in KYSE510 and TE-1 cells was detected by RNA pull-down and RIP. G) Actinomycin D treatment assessed the stability of GBX2 mRNA after EIF4A3 knockdown. H) By knocking down circ_0021727, the binding relationship between GBX2 and EIF4A3 in ESCC cells was tested by RIP. I) Overexpressed circ_0021727 and knocked down EIF4A3 in ESCC cells, the stability of GBX2 mRNA was detected using actinomycin D. n=3/group; *p<0.05, **p<0.01, p<0.001

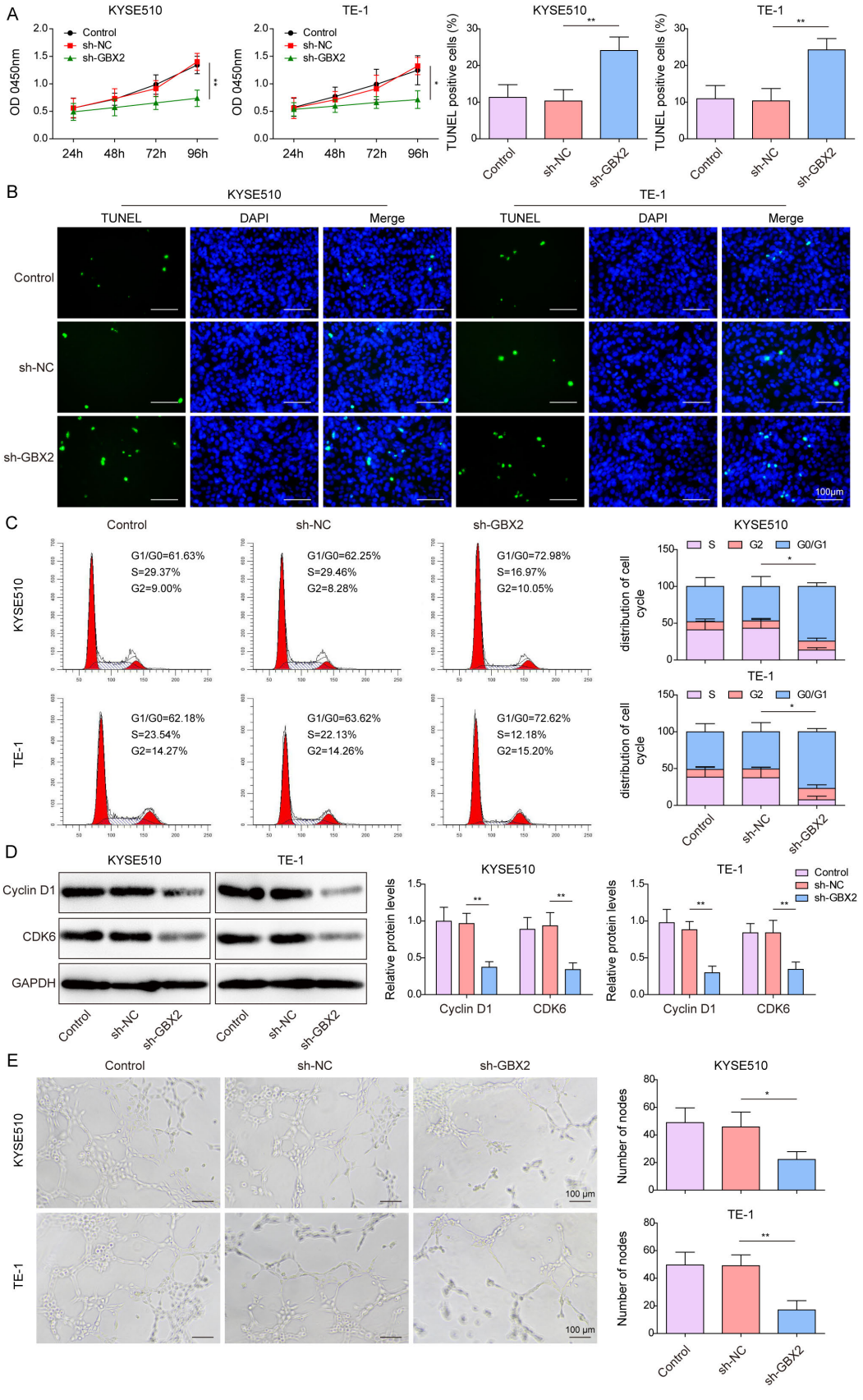

Figure 4. Knockdown of GBX2 induced G0/G1 phase arrest, promoted apoptosis, and inhibited angiogenesis in ESCC cells. A) The viability of ESCC cells after GBX2 knockdown was assessed by CCK-8 reagent. B) After GBX2 knockdown, apoptosis of ESCC cells was detected by TUNEL. The bar graph displayed the statistics of the percentage of TUNEL-positive cells. Scale bar = 100 μm C) The ESCC cell cycle after knockdown of GBX2 was characterized using flow cytometry. D) Western blot was used to evaluate the expression of cyclin D1 and CDK6 in ESCC cells after knocking down the GBX2 gene. E) The angiogenesis of HUVECs was examined using a tubule formation assay. Scale bar = 100 μm; n=3/group; *p<0.05, **p<0.01, p<0.001

fected KYSE510 and TE-1 cells with sh-GBX2 to knock down GBX2 (Supplementary Figure S3D). The level of GBX2 in the sh-GBX2 group was clearly reduced (Supplementary Figures S3E, S3F). At the same time, GBX2 knockdown significantly reduced the viability of ESCC cells (Figure 4A). Also, TUNEL experiments showed that knocking down GBX2 promoted the apoptosis of ESCC cells (Figure 4B). Moreover, the knockdown of GBX2 increased the proportion of KYSE510 and TE-1 cells in the G0/G1 phase, inhibiting the cell cycle transition from G1 to S (Figure 4C). Besides, cyclin D1 and CDK6 were downregulated after knockdown of GBX2 (Figure 4D). Meanwhile, GBX2 knockdown also resulted in inhibition of HUVECs angiogenesis (Figure 4E). Overall, knocking down GBX2 induced ESCC cells G0/G1 arrest, promoted apoptosis, and inhibited endothelial cell angiogenesis.

GBX2 overexpression reversed the effect of circ_0021727 knockdown on ESCC progression. To investigate whether circ_0021727 promotes ESCC by regulating GBX2, we first overexpressed GBX2 in ESCC cells (Supplementary Figures S3G–S3I). As shown in Supplementary Figures S3J and S3K, the knockdown of circ_0021727 significantly reduced GBX2 levels, and overexpression of GBX2 restored their expression. In addition, knocking down circ_0021727 inhibited the viability of ESCC cells and promoted cell apoptosis, while overexpressing GBX2 could reverse this phenomenon (Figures 5A, 5B). Also, the knockdown of circ_0021727 resulted in ESCC cell arrest in the G0/G1 phase, which was offset by the overexpression of GBX2 (Figure 5C). At the same time, GBX2 overexpression could restore the dysregulation of cyclin D1 and CDK6 expression caused by circ_0021727 knockdown (Figure 5D). More importantly, the knockdown of circ_0021727 inhibited HUVECs angiogenesis, and overexpression of GBX2 reversed this effect (Figure 5E). Therefore, circ_0021727 promoted ESCC progression by upregulating GBX2.

Overexpression of GBX2 reversed the effect of circ_0021727 knockdown on ESCC tumor growth *in vivo*. As shown in Figure 6A, it was clearly observed that knockdown of circ_0021727 inhibited tumor growth compared to Control and sh-NC+oe-NC groups, whereas further overexpression of GBX2 promoted tumor growth. Knockdown of circ_0021727 inhibited tumor growth rate, which was reversed by further overexpression of GBX2 (Figure 6B). Meanwhile, the knockdown of circ_0021727 also reduced tumor weight, and overexpression of GBX2 reversed the effect of the knockdown of circ_0021727 (Figure 6C). In addition, the knockdown of circ_0021727 decreased the expression of Ki-67, a marker of cell proliferation, whereas overexpression of GBX2 increased the expression of Ki-67 (Figure 6D). Meanwhile, the knockdown of circ_0021727 decreased the expression of the angiogenic marker CD31, while overexpression of GBX2 reversed the effect of the knockdown of circ_0021727 (Figure 6D). Knockdown of circ_0021727 downregulated the protein levels of GBX2, cyclin D1, and CDK6, while overexpression of GBX2 reversed the levels of the above proteins (Figure 6E). Therefore, circ_0021727 promoted ESCC tumor growth via upregulating GBX2 *in vivo*.

Discussion

ESCC is a major challenge to global health, and its high morbidity and mortality make it the focus of global health attention [20]. In the past few decades, due to the lack of a validated diagnostic and prognostic landmark has made early-stage ESCC difficult to detect, with poor treatment effects and low overall five-year survival [21]. Therefore, a compelling urgency to discover new biological targets has been established. We have previously reported that circ_0021727 enhanced the invasion, migration, and proliferation of ESCC cells [9]. However, the role of circ_0021727 in other malignant phenotypes of ESCC cells is worth further exploration, and the specific mechanism by which circ_0021727 may serve as a biomarker of ESCC requires further investigation. Malignant tumor phenotype is not only related to tumor cell proliferation, invasion, and migration but also to tumor cell cycle arrest, apoptosis, and angiogenesis [22]. Angiogenesis, the formation of new blood vessels from existing blood vessels on top of existing ones, is considered a key process for tumor cell proliferation and metastasis [20]. The rapid proliferation and growth of cancer cells are driven by an accelerated cell cycle progression [23]. In this study, we found that circ_0021727 reduced the G0/G1 phase arrest of ESCC cells, inhibited apoptosis, and promoted endothelial cell angiogenesis. Mechanically, circ_0021727 promoted ESCC cell progression by recruiting EIF4A3 to stabilize GBX2 mRNA.

Studies have demonstrated that circRNAs are strongly associated with tumor cell proliferation, cycle arrest, and angiogenesis [24, 25]. For example, hsa_circ_0000519 was able to promote angiogenesis in hepatocellular carcinoma through the miR-1296/E2F7 axis and inhibit cell cycle arrest in the G0/G1 phase [25]. In addition, circRNAs are widely involved in the regulation of ESCC processes [26–28]. For instance, circ_0001821 affected cell cycle arrest in ESCC cells [26]. Guo et al. found that hsa_circ_0000417 depletion promoted apoptosis and cell cycle arrest at the G0/G1 phase in ESCC cells [27]. In our study, circ_0021727 was highly expressed in ESCC cells, and knockdown circ_0021727 significantly reduced the viability and promoted apoptosis of ESCC cells, while overexpression of circ_0021727 had the opposite effect. CDK6 protein is a key component of the protein kinase complex, and its role is critical in speeding up the transition from the G1 to the S phase of the cell cycle, a crucial phase for cell proliferation [29]. Moreover, CDK6 is regulated by cyclin D1 [30]. Herein, overexpression of circ_0021727 upregulated cyclin D1 and CDK6 expression, alleviated the arrest of ESCC cells in the G0/G1 phase, and promoted the transition of ESCC cells to the S phase. At the same time, angiogenesis is one of the important processes of tumor cell proliferation [20]. We found that circ_0021727

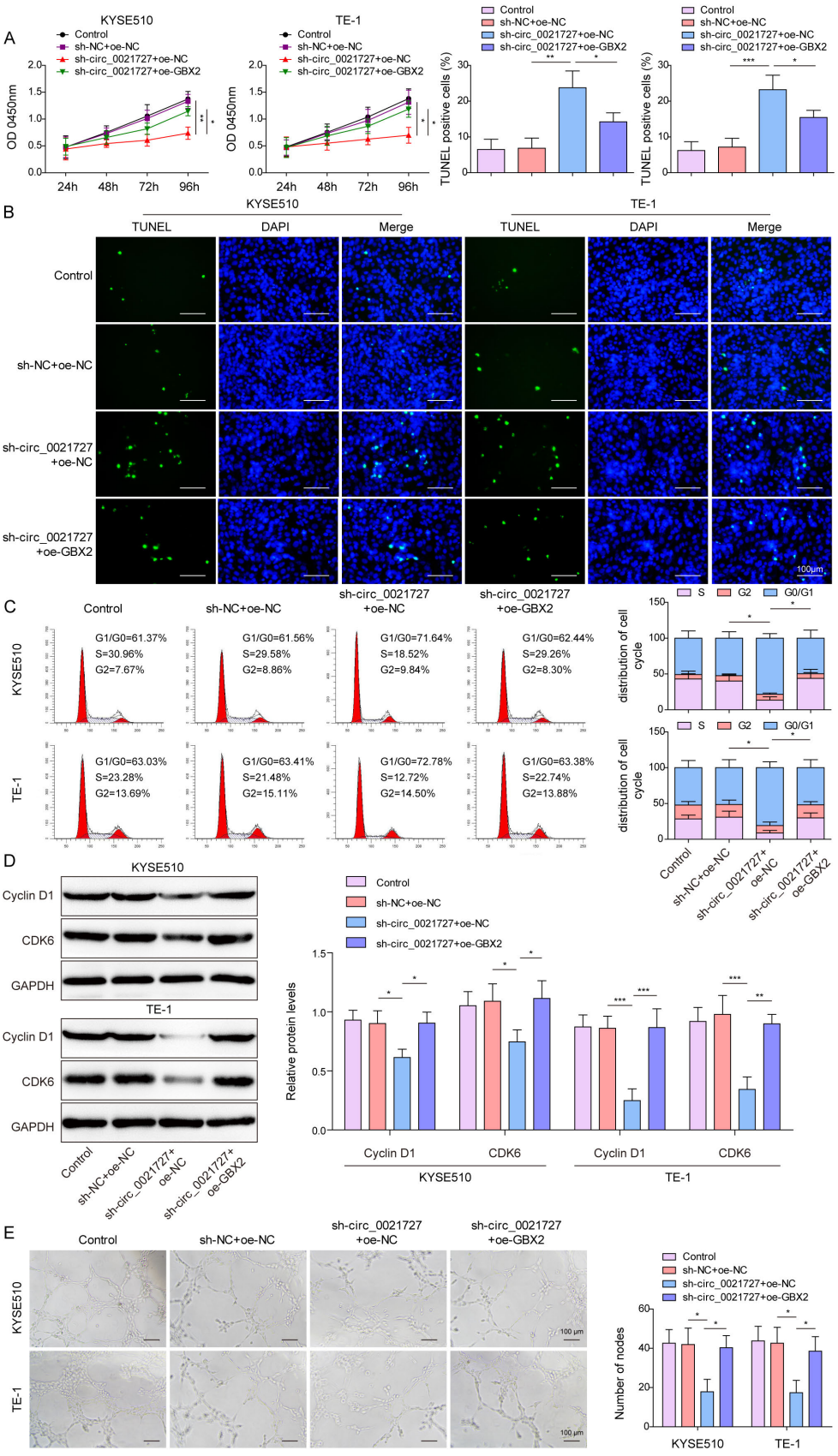

Figure 5. GBX2 overexpression reversed the effect of circ_0021727 knockdown on ESCC progression. A) The viability of cells was assessed using the CCK-8 assay after knockdown of circ_0021727 and overexpressing the GBX2. B) TUNEL assay was used to analyze the apoptosis of ESCC cells after knockdown of circ_0021727 and overexpression of GBX2. The bar graph displayed the statistics of the percentage of TUNEL-positive cells. Scale bar = 100 μm C) After knocking down circ_0021727 or overexpressing GBX2 in ESCC cells, the distribution of G0/G1, S, and G2/M phases of the cell cycle was analyzed by flow cytometry. D) Cyclin D1 and CDK6 expression in ESCC cells with knockdown of circ_0021727 or overexpression of GBX2 were detected by western blot. E) KYSE510 and TE-1 cells with knock-down circ_0021727 and overexpression of GBX2 were co-cultured with HUVECs, and a tubule formation assay was used to test the tubular capacity of HUVECs. Scale bar = 100 μm; n=3/group; *p<0.05, **p<0.01, p<0.001

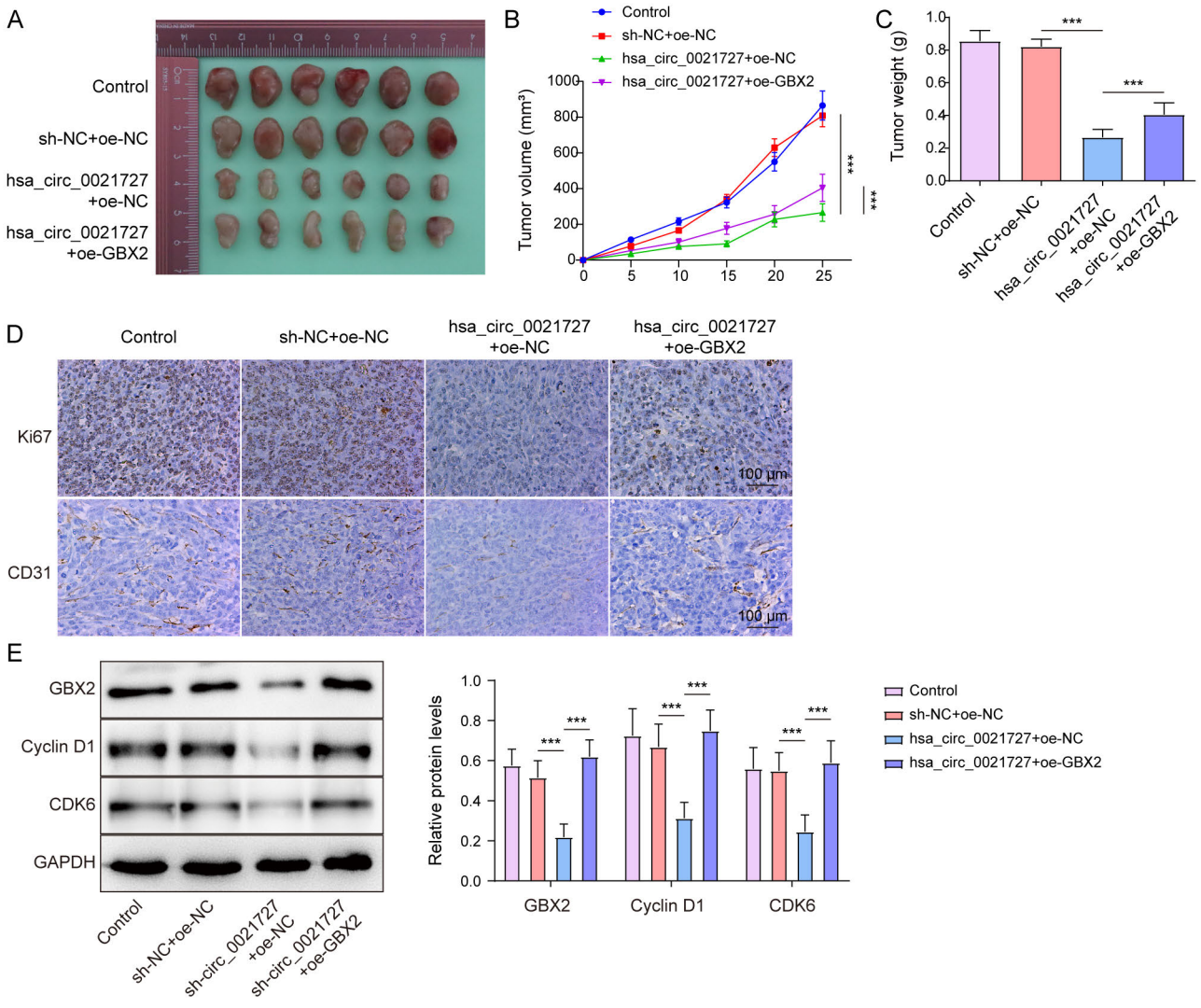

Figure 6. Overexpression of GBX2 reversed the effect of circ_0021727 knockdown on ESCC tumor growth *in vivo*. KYSE510 cell lines with the stable knockout of hsa_circ_0021727 and overexpression of GBX2 were subcutaneously injected into BALB/C nude mice. A) Tumor morphology diagram (n=6). B) Tumor growth curve. Tumor volume was recorded every 5 days after seeding (n=6). C) Weight of the tumor (n=6). D) The expression of Ki-67 and angiogenesis marker CD31 was detected by IHC (n=3). Scale bar = 100 μm. E) The GBX2 and cycle-related proteins (cyclin D1 and CDK6) were measured by western blot (n=3). *p<0.05, **p<0.01, p<0.001

induced endothelial cell angiogenesis. The above results suggested that circ_0021727 promoted cell cycle progression and angiogenesis and inhibited apoptosis in ESCC cells, thereby promoting the progression of ESCC.

Previous research has indicated that GBX2 is a cancer-promoting factor that can affect the proliferation, migration, invasion, and angiogenesis of cancer cells [15]. For example, Wang et al. found that GBX2 promoted lung cancer progression by regulating the AKT/ERK signaling pathway to enhance cell viability, invasion, and migration [15]. In our experiments, knocking down of GBX2 inhibited ESCC cell viability and angiogenesis and promoted ESCC cell arrest at the G0/G1 phase and apoptosis. What's more, our research revealed that GBX2 was the downstream molecule of the circ_0021727. Knockdown of the circ_0021727 reduced GBX2 expression, while circ_0021727 overexpression significantly increased GBX2 level. Moreover, overexpression of GBX2 reversed the inhibitory impact of knockdown circ_0021727 on ESCC cell cycle arrest, apoptosis induction, and angiogenesis. Knockdown of circ_0021727 inhibited tumor growth *in vivo*, while further overexpression of GBX2 reversed this inhibitory effect. Therefore, circ_0021727-regulated GBX2 performed a significant role in facilitating the progression of ESCC.

CircRNA normally binds to RBPs to regulate downstream mRNA involved in cancer progression [31]. EIF4A3 is an RBP

that can modulate the stability of its downstream mRNAs via binding with circRNAs. For instance, hsa_circ_0068631 recruited EIF4A3 to increase the stability of c-Myc mRNA in breast cancer [32]. circETFA promoted the development of hepatocellular carcinoma by recruiting EIF4A3 to stabilize miR-612 [33]. Herein, our study demonstrated that there was a binding relationship between circ_0021727 and EIF4A3, EIF4A3 and GBX2. Additionally, knocking down EIF4A3 reduced the effect of circ_0021727 on GBX2 mRNA stability enhancement. Therefore, circ_0021727 promoted the stability of GBX2 mRNA by recruiting to EIF4A3. A growing body of research has suggested that circRNAs modulate mRNA expression through miRNA sponge, which plays important roles in cancer development, including ESCC [5, 34, 35]. For example, hsa_circ_0046534 acted as a sponge for miR-339-5p to promote the proliferation and metastasis of ESCC cells by upregulating matrix metalloproteinase 2 expression [34]. Our previous study discovered that circ_0021727 promoted ESCC progression by activating the TAB1/NF-κB pathway by targeting miR-23b-5p [9]. Although we excluded the possibility that circ_0021727 regulated GBX2 via sponging miR-23b-5p, whether circ_0021727 can regulate GBX2 mRNA levels by sponging other miRNAs deserves further study.

In summary, our results determined that circ_0021727 circ_0021727 plays a vital regulatory role in the ESCC cell cycle and angiogenesis. Mechanically, circ_0021727 promoted the progression of ESCC by recruiting EIF4A3 to increase the stability of GBX2 mRNA. Our findings provide a theoretical basis for circ_0021727 as a predictor and therapeutic target of ESCC.

Supplementary information is available in the online version of the paper.

Acknowledgement: This work was supported by Science and Technology Research Project of Jiangxi Provincial Department of Education (GJJ211530).

References

[1] ZHANG L, LI L, CHEN X, YUAN S, XU T et al. Evodiamine inhibits ESCC by inducing M-phase cell-cycle arrest via CUL4A/p53/p21 axis and activating noxa-dependent intrinsic and DR4-dependent extrinsic apoptosis. Phytomedicine 2023; 108: 154493. https://doi.org/10.1016/j.phymed.2022.154493

[2] YUAN Y, PING W, ZHANG R, HAO Z, ZHANG N. DEPDC1B collaborates with GABRD to regulate ESCC progression. Cancer Cell Int 2022; 22: 214. https://doi.org/10.1186/s12935-022-02593-z

[3] JIA J, LI H, CHU J, SHENG J, WANG C et al. LncRNA FAM83A-AS1 promotes ESCC progression by regulating miR-214/CDC25B axis. J Cancer 2021; 12: 1200–1211. https://doi.org/10.7150/jca.54007

[4] LIU B, ZHAO N, ZHOU Y, LU Y, CHEN W et al. Circular RNA circ_ABCB10 in cancer. Clin Chim Acta 2021; 518: 93–100. https://doi.org/10.1016/j.cca.2021.03.010

[5] LIU Z, ZHOU Y, LIANG G, LING Y, TAN W et al. Circular RNA hsa_circ_001783 regulates breast cancer progression via sponging miR-200c-3p. Cell Death Dis 2019; 10: 55. https://doi.org/10.1038/s41419-018-1287-1

[6] ZHOU J, WANG L, SUN Q, CHEN R, ZHANG C et al. Hsa_circ_0001666 suppresses the progression of colorectal cancer through the miR-576-5p/PCDH10 axis. Clin Transl Med 2021; 11: e565. https://doi.org/10.1002/ctm2.565

[7] Zhang Y, Li J, Cui Q, Hu P, Hu S et al. Circular RNA hsa_circ_0006091 as a novel biomarker for hepatocellular carcinoma. Bioengineered 2022; 13: 1988–2003. https://doi.org/10.1080/21655979.2021.2006952

[8] GONG W, XU J, WANG Y, MIN Q, CHEN X et al. Nuclear genome-derived circular RNA circPUM1 localizes in mitochondria and regulates oxidative phosphorylation in esophageal squamous cell carcinoma. Signal Transduct Target Ther 2022; 7: 40. https://doi.org/10.1038/s41392-021-00865-0

[9] MENG F, ZHANG X, WANG Y, LIN J, TANG Y et al. Hsa_circ_0021727 (circ-CD44) promotes ESCC progression by targeting miR-23b-5p to activate the TAB1/NFκB pathway. Cell Death Dis 2023; 14: 9. https://doi.org/10.1038/s41419-022-05541-x

[10] MENG L, ZHANG Y, WU P, LI D, LU Y et al. CircSTX6 promotes pancreatic ductal adenocarcinoma progression by sponging miR-449b-5p and interacting with CUL2. Mol Cancer 2022; 21: 121. https://doi.org/10.1186/s12943-022-01599-5

[11] MA J, ZHAO X, SHI L. Circ 003390/Eukaryotic translation initiation factor 4A3 promoted cell migration and proliferation in endometrial cancer via vascular endothelial growth factor signaling by miR-195-5p. Bioengineered 2022; 13: 11958–11972. https://doi.org/10.1080/21655979.2022.2069358

[12] SAKELLARIOU D, FRANKEL LB. EIF4A3: a gatekeeper of autophagy. Autophagy 2021; 17: 4504–4505. https://doi.org/10.1080/15548627.2021.1985881

[13] LUO P, GONG Y, WENG J, WEN F, LUO J et al. CircKIF4A combines EIF4A3 to stabilize SDC1 expression to activate c-src/FAK and promotes TNBC progression. Cell Signal 2023; 108: 110690. https://doi.org/10.1016/j.cellsig.2023.110690

[14] XU S, GE Y, WANG X, YIN W, ZHU X et al. Circ-USP9X interacts with EIF4A3 to promote endothelial cell pyroptosis by regulating GSDMD stability in atherosclerosis. Clin Exp Hypertens 2023; 45: 2186319. https://doi.org/10.1080/10641963.2023.2186319

[15] WANG Y, HUI J, LI R, FU Q, YANG P et al. GBX2, as a tumor promoter in lung adenocarcinoma, enhances cells viability, invasion and migration by regulating the AKT/ERK signaling pathway. J Gene Med 2020; 22: e3147. https://doi.org/10.1002/jgm.3147

[16] CHEN X, CHENG P, HU C. LncRNA FEZF1-AS1 accelerates the migration and invasion of laryngeal squamous cell carcinoma cells through miR-4497 targeting GBX2. Eur Arch Otorhinolaryngol 2021; 278: 1523–1535. https://doi.org/10.1007/s00405-021-06636-5

[17] GU H, ZHONG Y, LIU J, SHEN Q, WEI R et al. The Role of miR-4256/HOXC8 Signaling Axis in the Gastric Cancer Progression: Evidence From lncRNA-miRNA-mRNA Network Analysis. Front Oncol 2021; 11: 793678. https://doi.org/10.3389/fonc.2021.793678

[18] LIN YH, ZHANG BY, CHEN ZS. circRERE regulates the expression of GBX2 through miR-1299 and ZC3H13/N(6)-methyladenosine (m(6)A) to promote growth and invasion of hepatocellular carcinoma cells. J Biosci 2022; 47: 52.

[19] WANG X, LIU S, XU B, LIU Y, KONG P et al. circ-SIRT1 Promotes Colorectal Cancer Proliferation and EMT by Recruiting and Binding to eIF4A3. Anal Cell Pathol (Amst) 2021; 2021: 5739769. https://doi.org/10.1155/2021/5739769

[20] ZHANG Y, CHEN C, LIU Z, GUO H, LU W et al. PABPC1-induced stabilization of IFI27 mRNA promotes angiogenesis and malignant progression in esophageal squamous cell carcinoma through exosomal miRNA-21-5p. J Exp Clin Cancer Res 2022; 41: 111. https://doi.org/10.1186/s13046-022-02339-9

[21] LU Z, ZHENG S, LIU C, WANG X, ZHANG G et al. S100A7 as a potential diagnostic and prognostic biomarker of esophageal squamous cell carcinoma promotes M2 macrophage infiltration and angiogenesis. Clin Transl Med 2021; 11: e459. https://doi.org/10.1002/ctm2.459

[22] PENG J, SHI S, YU J, LIU J, WEI H et al. miR-378d suppresses malignant phenotype of ESCC cells through AKT signaling. Cancer Cell Int 2021; 21: 702. https://doi.org/10.1186/s12935-021-02403-y

[23] YUAN S, PAN Y, XU T, ZHANG L, CHEN X et al. Daurisoline Inhibits ESCC by Inducing G1 Cell Cycle Arrest and Activating ER Stress to Trigger Noxa-Dependent Intrinsic and CHOP-DR5-Dependent Extrinsic Apoptosis via p-eIF2α-ATF4 Axis. Oxid Med Cell Longev 2022; 2022: 5382263. https://doi.org/10.1155/2022/5382263

[24] KRISTENSEN LS, JAKOBSEN T, HAGER H, KJEMS J. The emerging roles of circRNAs in cancer and oncology. Nat Rev Clin Oncol 2022; 19: 188–206. http://doi.org/10.1038/s41571-021-00585-y

[25] LIU Y, TANG H, ZHANG Y, WANG Q, LI S et al. Circular RNA hsa_circ_0000519 contributes to angiogenesis and tumor progression in hepatocellular carcinoma through the miR-1296/E2F7 axis. Hum Cell 2023; 36: 738–751. https://doi.org/10.1007/s13577-022-00854-7

[26] LIN C, WEI Y, DUAN X, LIU C, DU Y et al. Circ_0001821 Affects Proliferation and the Cell Cycle in Esophageal Squamous Cell Carcinoma by Elevating BTRC-Mediated IKBA Ubiquitination. Mol Cancer Res 2022; 20: 1686–1696. https://doi.org/10.1158/1541-7786.Mcr-22-0023

[27] GUO S, WANG G, ZHAO Z, LI D, SONG Y et al. Deregulated expression and subcellular localization of CPSF6, a circRNA-binding protein, promote malignant development of esophageal squamous cell carcinoma. Chin J Cancer Res 2022; 34: 11–27. https://doi.org/10.21147/j.issn.1000-9604.2022.01.02

[28] ZHANG H, JU L, HU P, YE J, YANG C et al. Circular RNA 0014715 Facilitates Cell Proliferation and Inhibits Apoptosis in Esophageal Squamous Cell Carcinoma. Cancer Manag Res 2021; 13: 4735–4749. https://doi.org/10.2147/cmar.S314882

[29] LU K, LI B, ZHANG H, XU Z, SONG D et al. A novel silicone derivative of natural osalmid (DCZ0858) induces apoptosis and cell cycle arrest in diffuse large B-cell lymphoma via the JAK2/STAT3 pathway. Signal Transduct Target Ther 2020; 5: 31. https://doi.org/10.1038/s41392-020-0123-0

[30] XIA B, YANG S, LIU T, LOU G. miR-211 suppresses epithelial ovarian cancer proliferation and cell-cycle progression by targeting Cyclin D1 and CDK6. Mol Cancer 2015; 14: 57. https://doi.org/10.1186/s12943-015-0322-4

[31] LIANG Y, WANG H, CHEN B, MAO Q, XIA W et al. circDCUN1D4 suppresses tumor metastasis and glycolysis in lung adenocarcinoma by stabilizing TXNIP expression. Mol Ther Nucleic Acids 2021; 23: 355–368. https://doi.org/10.1016/j.omtn.2020.11.012

[32] WANG X, CHEN M, FANG L. hsa_circ_0068631 promotes breast cancer progression through c-Myc by binding to EIF4A3. Mol Ther Nucleic Acids 2021; 26: 122–134. https://doi.org/10.1016/j.omtn.2021.07.003

[33] HUANG X, TAN W, LIU Z, FU X, LI Z et al. EIF4A3-induced circZFAND6 promotes breast cancer proliferation and metastasis through the miR-647/FASN axis. Life Sci 2023; 324: 121745. https://doi.org/10.1016/j.lfs.2023.121745

[34] XU T, HU Y, ZHAO Y, QI Y, ZHANG S et al. Hsa_circ_0046534 accelerates esophageal squamous cell carcinoma proliferation and metastasis via regulating MMP2 expression by sponging miR-339-5p. Cell Signal 2023; 112: 110906. https://doi.org/10.1016/j.cellsig.2023.110906

[35] LONG F, LI L, XIE C, MA M, WU Z et al. Intergenic CircRNA Circ_0007379 Inhibits Colorectal Cancer Progression by Modulating miR-320a Biogenesis in a KSRP-Dependent Manner. Int J Biol Sci 2023; 19: 3781–3803. https://doi.org/10.7150/ijbs.85063

https://doi.org/10.4149/neo_2024_240604N243

hsa_circ_0021727 facilitates esophageal squamous cell carcinoma progression by stabilizing GBX2 mRNA through interacting with EIF4A3

Jie LIN[1], Qiuping ZHU[1], Fanlin ZENG[2,*]

Supplementary Information

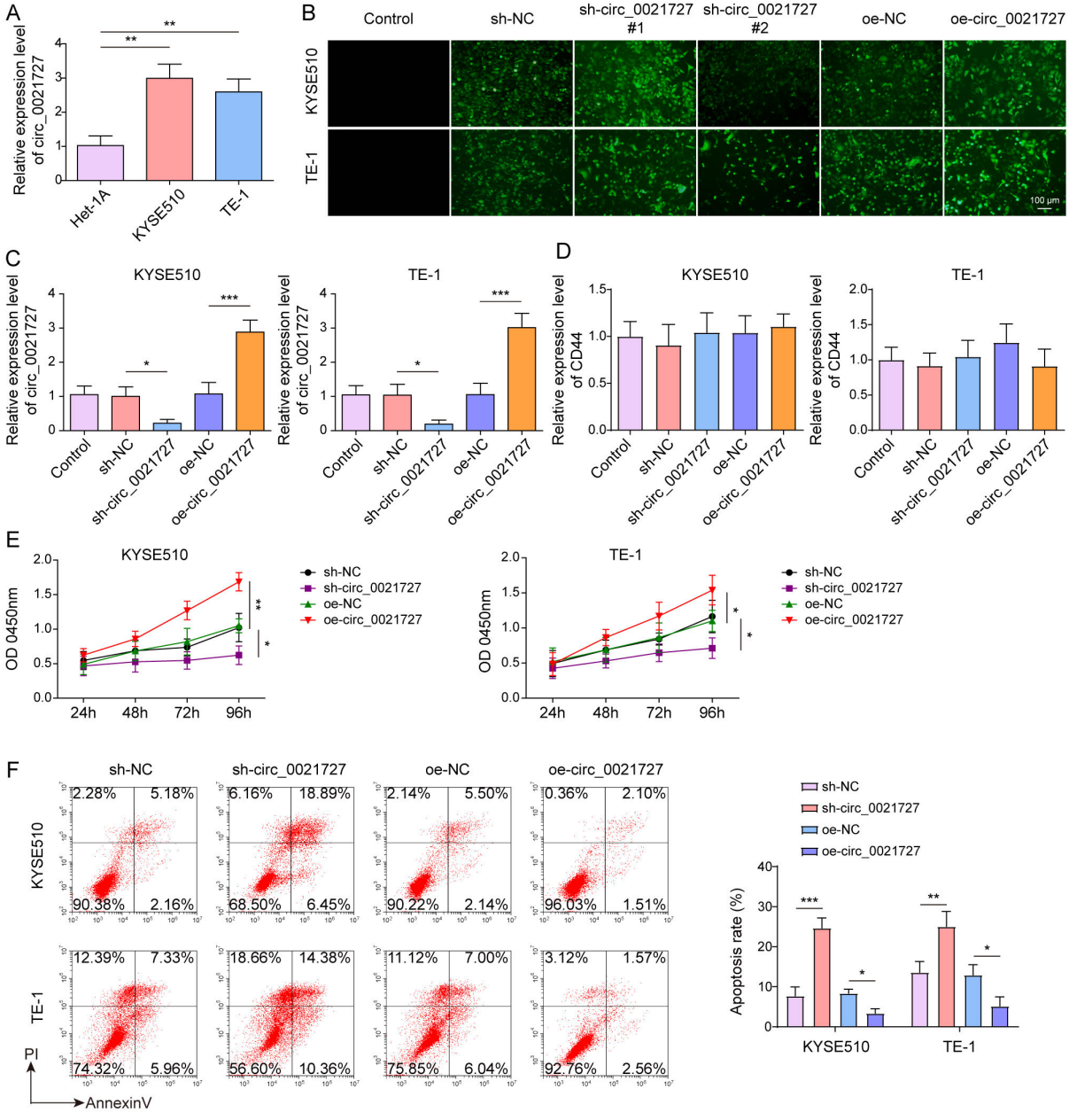

Supplementary Figure S1. circ_0021727 promoted proliferation and inhibited apoptosis in ESCC. A) The levels of circ_0021727 in Het-1A, KYSE510 and TE-1 cells were measured by RT-qPCR. B) The transfection effect of sh-NC, sh-circ_0021727, oe-NC, oe-circ_0021727 was detected by fluorescence microscopy. C) RT-qPCR was used to detect circ_0021727 levels after knockdown or overexpression of circ_0021727 in ESCC cells. D) RT-qPCR was used to detect CD44 levels after knockdown or overexpression of circ_0021727 in ESCC cells. E) CCK-8 assay was performed to detect the influence of knockdown and overexpression of circ_0021727 on ESCC cell viability. F) Apoptosis was detected by flow cytometry. n=3/group; *p<0.05, **p<0.01, p<0.001

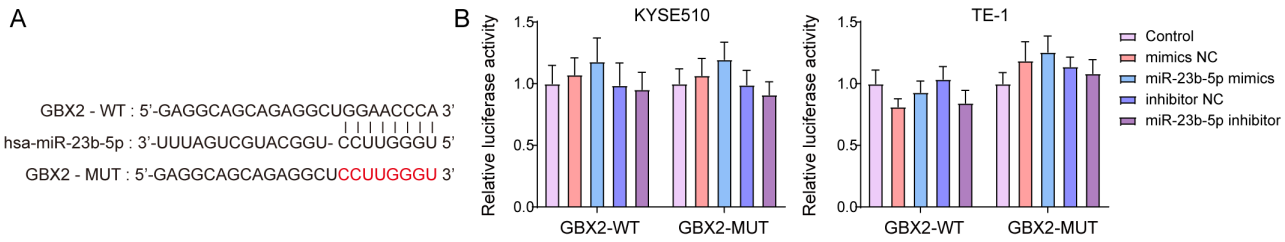

Supplementary Figure S2. The detection of miR-23b-5p and GBX2 mRNA binding relationship. A) TargetScan database predicted the binding sites of miR-23b-5p and GBX2 mRNA. B) Binding of miR-23b-5p and GBX2 mRNA was detected by a dual luciferase reporter gene. n=3

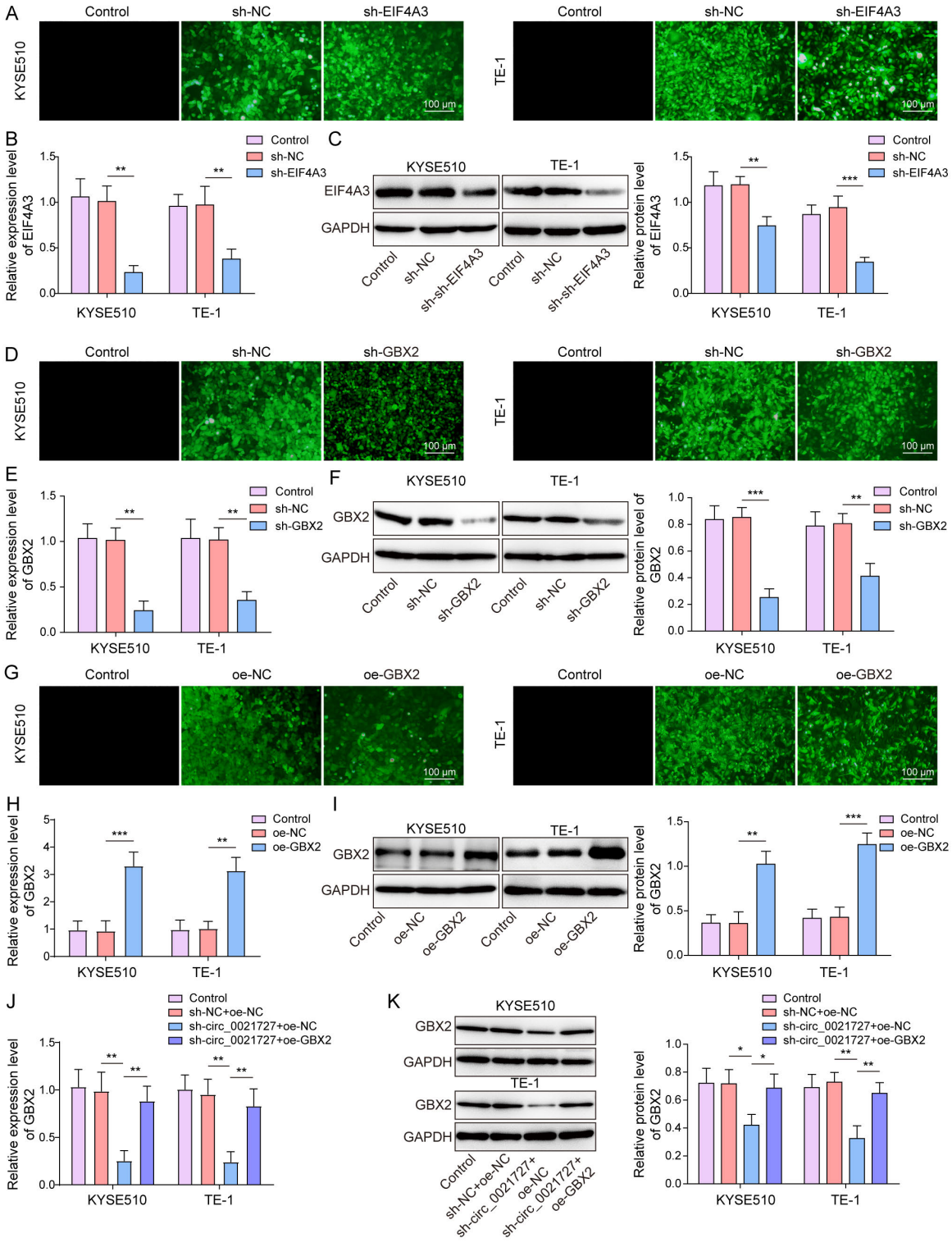

Supplementary Figure S3. EIF4A3 and GBX2 interference plasmid transfection and expression level detection. A) The transfection effect of sh-EIF4A3 was detected by fluorescence microscopy. B, C) After knockdown of EIF4A3, the expression levels of EIF4A3 in ESCC cells were analyzed using RT-qPCR and Western blot techniques, respectively. D) The transfection effect of sh-NC, sh-circ_0021727, oe-NC, oe-circ_0021727 was detected by fluorescence microscopy. E, F) GBX2 knockdown effect were assessed through RT-qPCR and Western blot in ESCC cells. G) The transfection effect of oe-GBX2 was detected by fluorescence microscopy. H, I) GBX2 overexpression effect was assessed by RT-qPCR and Western blot in ESCC cells. J, K) The expression of GBX2 after knockdown of circ_0021727 or/and overexpression of GBX2 were examined by RT-qPCR and Western blot in ESCC cells. n=3/group; *p<0.05, **p<0.01, p<0.001